

# Thermal and kinetic study of dehydration and decomposition processes for copper intercalated $\gamma$ -zirconium and $\gamma$ -titanium phosphates

Stefano Vecchio<sup>a,\*</sup>, Romolo Di Rocco<sup>b</sup>, Carla Ferragina<sup>b</sup>, Stefano Materazzi<sup>c</sup>

<sup>a</sup> *Dipartimento di Ingegneria Chimica, dei Materiali, delle Materie Prime e Metallurgia, Università di Roma "La Sapienza", Via del Castro Laurenziano 7, 00161 Roma, Italy*

<sup>b</sup> *CNR, Istituto di Metodologie Inorganiche e dei Plasmi, Via Salaria km. 29.300, 00016 Monterotondo, Roma, Italy*

<sup>c</sup> *Dipartimento di Chimica, Università di Roma "La Sapienza", P.le A. Moro 5, 00185 Roma, Italy*

Received 10 January 2005; received in revised form 28 April 2005; accepted 29 April 2005

Available online 1 July 2005

## Abstract

Thermal dehydration and decomposition processes of some intercalation compounds were studied by simultaneous TG/DSC and evolved gas analysis (EGA).  $\gamma$ -Zirconium and  $\gamma$ -titanium phosphates were intercalated with 1,10-phenanthroline and subsequently reacted with copper ions to form the complex in situ. Reaction mechanisms for thermal decomposition of all the materials were investigated and proposed according to the mass losses recorded by TG and confirmed by EGA (TG–FTIR). The Ozawa–Flynn–Wall isoconversional method provided dependencies of activation energy on the degree of conversion. A “single point” model-free method was also applied using Kissinger equation and the derived results were compared to those of the former method.

© 2005 Elsevier B.V. All rights reserved.

**Keywords:** Ion-exchangers; Intercalation compounds; Copper–phenanthroline complex; TG–DSC; X-ray powder diffraction; Ozawa–Flynn–Wall method; Kissinger method; TG–FTIR; EGA

## 1. Introduction

Inorganic ion-exchangers with a layered structure belonging to the class of acid phosphates of tetravalent elements [Me(IV)(HPO<sub>4</sub>)<sub>2</sub>·nH<sub>2</sub>O; Me = Zr, Ti, Sn; n = 1, 2, ...] are of interest due to their ability to exchange transition metal ions (t.m.i.) [1] and to intercalate organic molecules between the layers [2]. Organic intercalation materials can co-ordinate t.m.i. to obtain complexes formed in situ between the layers of the material [3]. These materials have potential application in the heterogeneous catalysis due to its chemical and thermal stability [4]. The most studied are the gamma phases of zirconium phosphate [ $\gamma$ -Zr(PO<sub>4</sub>)(H<sub>2</sub>PO<sub>4</sub>)·2H<sub>2</sub>O ( $\gamma$ -ZrP)] and titanium phosphate [ $\gamma$ -Ti(PO<sub>4</sub>)(H<sub>2</sub>PO<sub>4</sub>)·2H<sub>2</sub>O ( $\gamma$ -TiP)]. These materials are able to intercalate 1,10-phenanthroline (phen) and subsequently to exchange copper ions to give phenCu complex formed in situ [5].

To the best of our knowledge, no relevant information is available on the decomposition kinetics of phen intercalated as such or as a complex in these materials. The aim of this investigation is to show the influence of the exchanger on the thermal stability of the phenCu complex as well as to study the dehydration and decomposition processes for all the materials. The mechanisms of these processes were obtained by simultaneous TG/DSC techniques, and the activation energy was determined by means of two model-free methods, the isoconversional Ozawa–Flynn–Wall (OFW) and the single point Kissinger method.

## 2. Theory

Heterogeneous solid-state reactions can empirically be described by a single-step kinetic equation

$$\frac{d\alpha}{dt} = k(T)f(\alpha) \quad (1)$$

\* Corresponding author. Tel.: +39 06 49766906; fax: +39 06 49766749.  
E-mail address: [stefano.vecchio@uniroma1.it](mailto:stefano.vecchio@uniroma1.it) (S. Vecchio).

where  $t$  is the time,  $T$  the temperature,  $\alpha$  the extent of conversion and  $f(\alpha)$  is the reaction model. Mathematical expressions for several functional forms of the reaction model,  $f(\alpha)$ , are given in refs. [6–8]. Replacing  $k(T)$  with the Arrhenius equation gives

$$\frac{d\alpha}{dt} = A \exp\left(\frac{-E}{RT}\right) f(\alpha) \quad (2)$$

where  $A$  (the pre-exponential factor) and  $E$  (the activation energy) are the Arrhenius parameters and  $R$  is the gas constant. For non-isothermal experiments carried out with linear heating rates  $\beta$ , the reaction rate  $d\alpha/dt$  in Eq. (2) is replaced with  $\beta(d\alpha/dT)$  giving

$$\frac{d\alpha}{dT} = \left(\frac{A}{\beta}\right) \exp\left(\frac{-E}{RT}\right) f(\alpha) \quad (3)$$

Force-fitting experimental data to different model functions  $f(\alpha)$  is denoted as model-fitting methods [7,8]. After the  $f(\alpha)$  model has been selected from the best linear fit (assumed linear a priori) for a series of temperatures,  $k(T)$  is evaluated. Model-fitting methods can be misleading, especially in the case of non-isothermal experiments at single heating rate because they do not provide independent information on both  $k(T)$  and  $f(\alpha)$ . Several  $f(\alpha)$  models can fit data with Arrhenius parameters that can vary remarkably [9,10].

Model-free isoconversional methods allow for estimating the activation energy as a function of  $\alpha$  without choosing the reaction model. The basic assumption of these methods is that the reaction rate at constant extent of conversion  $\alpha$  depends only on the temperature [11]. Hence, constant  $E$  values can be expected in the case of single stage decompositions, while for multi-step processes  $E$  varies with  $\alpha$  due to the variation in the relative contributions of single steps to the overall reaction rate [12].

Among the model-free isoconversional methods that use linear procedures (in which kinetic parameters are derived from the slope of straight lines) one of the most reliable is the Ozawa–Flynn–Wall method [13,14]. According to this method, which is based on an integral form of Eq. (1), for a set of non-isothermal TG experiments carried out at different constant heating rates  $\beta$ , the activation energy at any particular value of  $\alpha$  is determined by the following equation:

$$(\ln \beta)_\alpha \approx \ln\left(\frac{AE}{R}\right)_\alpha - \ln g(\alpha) - 5.3305 - 1.052\left(\frac{E}{RT}\right)_\alpha \quad (4)$$

from the slope of the straight line obtained by plotting  $\ln \beta$  versus  $1/T$ . Errors may be introduced into the calculation of activation energy from Eq. (4) by the fact that Doyle's linear approximation

$$\ln p(x) \approx -5.3305 - 1.052x \quad (5)$$

where  $x = E/RT$  is valid only in the range  $20 \leq x \leq 60$ . Corrections of the temperature integral  $p(x)$  due to non-linearity of Eq. (5) have been proposed [15].

Kissinger [16,17] and others [18,19] have found that the peak temperature is a function of the heating rate through the following (pseudo) first-order reaction:

$$\ln\left(\frac{\beta}{T_m^2}\right) = \frac{-E}{RT_m} + \ln\left(\frac{AR}{E}\right) \quad (6)$$

where  $T_m$  is temperature that corresponds to the maximum of  $d\alpha/dT$ . This “model-free” kinetic method can be applied as a reasonable approximation regardless of order, providing a single  $E$  value. For this reason, it is often defined as “single point” method. If the reaction proceeds under conditions where thermal equilibrium is always maintained, then a plot of  $\ln(\beta/T_m^2)$  versus  $1/T_m$  gives a straight line with a slope equal to  $-E/R$ .

### 3. Experimental

#### 3.1. Chemicals

The copper acetate, zirconyl chloride, titanium oxide, phosphoric acid and 1,10-phenanthroline were purchased reagent grade from Aldrich and used without further purification.

#### 3.2. Materials

$\gamma$ -ZrP and  $\gamma$ -TiP were prepared as reported in [20,21]. The intercalation compounds obtained with 1,10-phenanthroline ( $\gamma$ -ZrPphen and  $\gamma$ -TiPphen) were prepared as reported in literature [22,23]. The copper complexes formed in situ ( $\gamma$ -ZrPphenCu and  $\gamma$ -TiPphenCu) are prepared as reported in [5]. Intercalation of phen and formation of phenCu complex between the layer of the exchanger evidenced by X-ray photoelectron spectroscopic measurements in [24] are outlined in Fig. 1.

#### 3.3. Physical measurements and chemical analysis

Copper ions were determined in the supernatant solutions, before and after contact with the exchangers with a GBC 903 A.A. spectrophotometer.

Phosphates were determined colorimetrically [25]. Water and the diamine contents and the thermal behavior of the materials were determined with a simultaneous TG/DTA Stanton Redcroft 1500 thermoanalyzer, Pt crucibles, heating rate  $10^\circ\text{C min}^{-1}$ , calcined up to  $1100^\circ\text{C}$  to constant weight in an airflow. X-ray powder diffraction (XRPD) was used to study phase changes in the materials by monitoring the  $d$  reflection and its harmonics. A Philips diffractometer (model PW 1130/00) was used with Ni-filtered Cu  $K\alpha$  radiation ( $\lambda = 1.541 \text{ \AA}$ ).

#### 3.4. TG/DSC and EGA measurements

The TG/DSC experimental measurements were carried out on a Stanton Redcroft 625 simultaneous TG/DSC con-

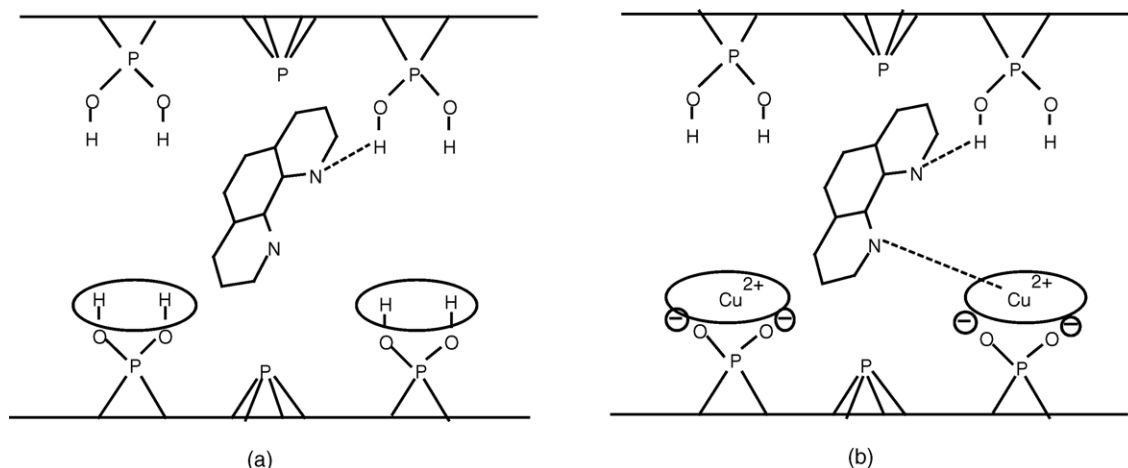


Fig. 1. Possible arrangements of phen (a) and phenCu complex (b) between the layers of the  $\gamma$ -ZrP exchanger.

nected to a 386 IBM-compatible personal computer. The calibration of this instrument was performed with very pure standards (indium, lead, tin, zinc, naphthalene and benzoic acid). Samples of 5–7 mg were weighed into aluminium pans in an argon-filled dry box. The TG/DSC system was purged with air at  $100 \text{ ml min}^{-1}$ . Gases evolved were continuously removed and analysed by on-line FTIR to prove the proposed decomposition steps. Heating rates were 2, 4, 6 and  $8 \text{ K min}^{-1}$  and at least three runs were made for each material. Thermodynamic quantities were calculated with the Stanton-Redcroft Data Acquisition System, Trace 2, Version 4.

## 4. Results and discussion

### 4.1. Materials

The proposed formulas of the examined materials are summarized in Table 1.

### 4.2. XRPD

X-ray powder diffraction patterns for  $\gamma$ -ZrP,  $\gamma$ -ZrPphen,  $\gamma$ -ZrPphenCu,  $\gamma$ -TiP,  $\gamma$ -TiPphen and  $\gamma$ -TiPphenCu at room temperature are given in Fig. 2. The first reflection  $d$  due to the layered structure of these materials (Table 1) increases from  $12.30 \text{ \AA}$  ( $\gamma$ -ZrP) to  $18.50 \text{ \AA}$  ( $\gamma$ -ZrPphen) due to intercalation of phen. The material  $\gamma$ -ZrPphenCu obtained after exchange with Cu ions shows two reflections:  $15.29$  and  $14.37 \text{ \AA}$ . The comparison of XRPD patterns of  $\gamma$ -TiP and  $\gamma$ -TiPphen also

shows the increase of  $d$  from  $11.70$  to  $17.50 \text{ \AA}$ .  $\gamma$ -TiPphenCu shows a single peak at  $17.30 \text{ \AA}$ .

After thermal treatment at  $220^\circ\text{C}$ , the  $d$  of  $\gamma$ -ZrPphen decreases from  $18.50$  to  $14.34 \text{ \AA}$ , while an increase to  $15.05 \text{ \AA}$  is found when the sample is treated at  $400^\circ\text{C}$ . For  $\gamma$ -ZrPphenCu treated at  $220^\circ\text{C}$  no differences from the data at room temperature are observed. A single value of  $15.00 \text{ \AA}$  is found for samples treated at  $400^\circ\text{C}$ . For  $\gamma$ -TiPphen treated at  $220^\circ\text{C}$ ,  $d$  values of  $17.32$  and  $15.30 \text{ \AA}$ , and at  $400^\circ\text{C}$  a single  $d = 15 \text{ \AA}$  are shown.  $\gamma$ -TiPphenCu behaves as its precursor; at  $220^\circ\text{C}$  a structure with two  $d$  reflections,  $17.30$  and  $15.29 \text{ \AA}$ , is observed; at  $400^\circ\text{C}$  a single phase is present with  $d = 15.40 \text{ \AA}$ .

### 4.3. TG/FTIR analysis

TG/FTIR results established that only dehydration processes occurred in the range  $298$ – $723 \text{ K}$  for all the materials. The EGA of all the compounds clearly shows that only water is released as a consequence of the TG step, with no other bands.

### 4.4. Thermal and kinetic analysis

#### 4.4.1. 1,10-Phenanthroline

TG/DTG and DSC curves of phen are shown in Fig. 3. Dehydration occurs at  $300$ – $370 \text{ K}$ . A sharp endotherm due to melting ( $\Delta H_{\text{fus}} = 10.7 \pm 0.6 \text{ kJ mol}^{-1}$ ) occurs at  $390$ – $396 \text{ K}$  up to about  $540 \text{ K}$ . Vaporization enthalpy  $81 \pm 3 \text{ kJ mol}^{-1}$ , is slightly higher than the activation energy of vaporization,  $78.3 \pm 0.4 \text{ kJ mol}^{-1}$ , obtained by the Kissinger method.  $E$  values ranged between  $80$  and  $87 \text{ kJ mol}^{-1}$  are calculated via the OFW method (Table 2).

#### 4.4.2. $\gamma$ -ZrPphen

Fig. 4 shows three dehydration steps for  $\gamma$ -ZrPphen in the range  $290$ – $480 \text{ K}$ . The fourth mass loss, between  $500$  and  $630 \text{ K}$ , is due to residual coordination water and condensa-

Table 1  
Chemical composition and interlayer distances of the examined materials

Materials		$d$ ( $\text{\AA}$ )
$\gamma$ -ZrPphen	$\gamma\text{-Zr}(\text{PO}_4)(\text{H}_2\text{PO}_4)\text{phen}_{0.50}\cdot 3\text{H}_2\text{O}$	18.50
$\gamma$ -ZrPphenCu	$\gamma\text{-Zr}(\text{PO}_4)(\text{HPO}_4)\text{phen}_{0.50}\text{Cu}_{0.50}\cdot 2.5\text{H}_2\text{O}$	14.37, 15.29
$\gamma$ -TiPphen	$\gamma\text{-Ti}(\text{PO}_4)(\text{H}_2\text{PO}_4)\text{phen}_{0.50}\cdot 1.5\text{H}_2\text{O}$	17.50
$\gamma$ -TiPphenCu	$\gamma\text{-Ti}(\text{PO}_4)(\text{HPO}_4)\text{phen}_{0.50}\text{Cu}_{0.50}\cdot 1.7\text{H}_2\text{O}$	17.30

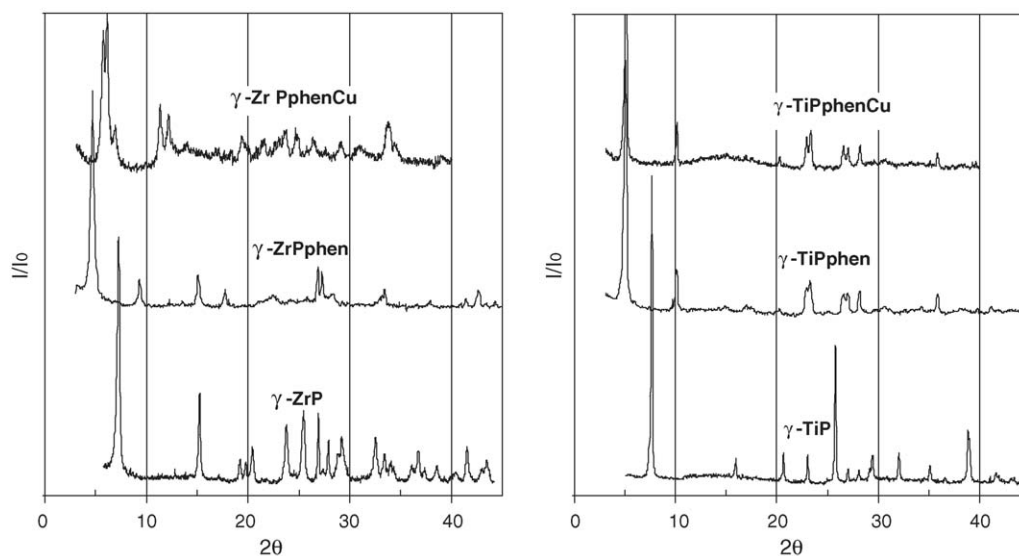


Fig. 2. XRPD patterns at room temperature.

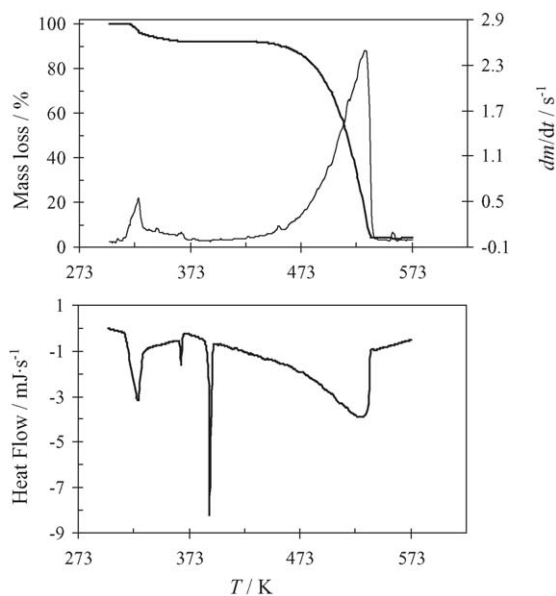
Fig. 3. TG/DTG and DSC curves of phen at 2 K min<sup>-1</sup> under a stream of air.

Table 2

$E_{\alpha}$  dependencies on the degree of conversion according to the OFW method for vaporization of phen

$\alpha$	$E_{\alpha}$ (kJ mol <sup>-1</sup> )	$\alpha$	$E_{\alpha}$ (kJ mol <sup>-1</sup> )
0.05	80 ± 4	0.55	83 ± 2
0.10	80 ± 3	0.60	84 ± 2
0.15	81 ± 3	0.65	85 ± 2
0.20	82 ± 1	0.70	85 ± 2
0.25	85 ± 3	0.75	86 ± 2
0.30	84 ± 3	0.80	87 ± 3
0.35	87 ± 3	0.85	87 ± 3
0.40	86 ± 2	0.90	87 ± 3
0.45	85 ± 2	0.95	86 ± 1
0.50	84 ± 2		

tion water of orthophosphate groups going to pyrophosphate groups. DTG peak temperatures are listed in Table 3 for comparison purposes. Only the first two dehydration steps were accompanied by endothermic effects in the DSC curve. Dehydration processes seem to be faster with increasing temperature (from the first to the fourth step). By contrast with pure phen, for which a vaporization process occurs, a single decomposition step takes place in the range 690–870 K with a very intense exothermic effect ( $-788 \pm 6$  kJ mol<sup>-1</sup>).  $E$  values around 190 kJ mol<sup>-1</sup> were found for this step with both kinetic methods.

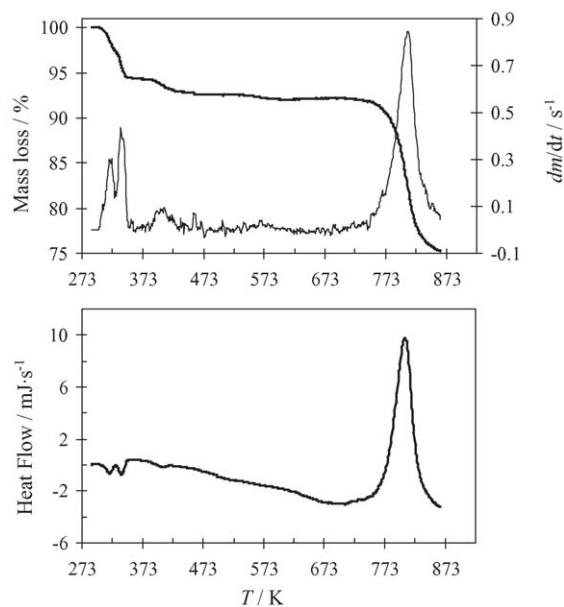
Fig. 4. TG/DTG and DSC curves of  $\gamma$ -ZrPphen at 2 K min<sup>-1</sup> under a stream of air.

Table 3  
DSC peak temperatures (at  $\beta = 2 \text{ K min}^{-1}$ ) and activation energies of dehydration and decomposition processes for  $\gamma\text{-ZrPphen}$

Step	Process	$T$ (K)	$E$ ( $\text{kJ mol}^{-1}$ )	
			From K method	From OFW method (range of $\alpha$ )
I	Dehydration	321.6	$82 \pm 3$	$77 \pm 5$ (0.05–0.20) $80 \pm 3$ (0.20–0.95)
II	Dehydration	337.7	$90 \pm 3$	$86 \pm 3$ (0.05–0.80) $72 \pm 7$ (0.80–0.95)
III	Dehydration	403.3	$108 \pm 5$	$88 \pm 9$ (0.05–0.20) $108 \pm 3$ (0.20–0.80)
IV	Dehydration	574.4	$137 \pm 6$	$139 \pm 5$ (0.05–0.95)
V	Decomposition	810.3	$192 \pm 5$	$181 \pm 8$ (0.05–0.20) $192 \pm 6$ (0.20–0.85) $184 \pm 5$ (0.85–0.95)

Temperature uncertainties are less than 0.5 K.

#### 4.4.3. $\gamma\text{-ZrPphenCu}$

Dehydration of  $\gamma\text{-ZrPphenCu}$  occurs in three steps up to 440 K (Fig. 5) (similarly to  $\gamma\text{-ZrPphen}$ ) with an overall mass loss of about 10% (about 8% for  $\gamma\text{-ZrPphen}$ ). DTG peak temperatures related to the second and third dehydration steps of  $\gamma\text{-ZrPphenCu}$  are higher than those of  $\gamma\text{-ZrPphen}$ . Similarly, the corresponding activation energies are higher, thus demonstrating that the presence of the phenCu complex hinders the loss of coordination and crystallization water. Conversely, the release of the condensation water to form the pyrophosphate groups (450–600 K) as well as the decomposition of phen (670–850 K) occurs at temperatures slightly lower (Fig. 5; Tables 3 and 4) with activation energies ranging between 130 and 150  $\text{kJ mol}^{-1}$ . A decomposition enthalpy much higher than that of  $\gamma\text{-ZrPphen}$  ( $-1247 \pm 11 \text{ kJ mol}^{-1}$ ) was found,

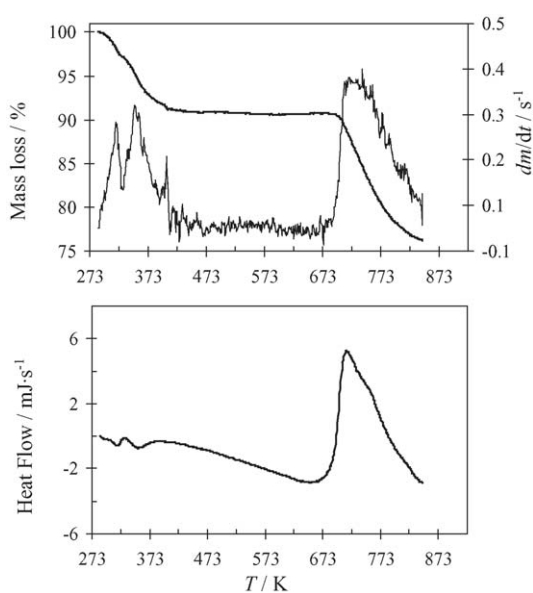


Fig. 5. TG/DTG and DSC curves of  $\gamma\text{-ZrPphenCu}$  at  $2 \text{ K min}^{-1}$  under a stream of air.

Table 4  
DSC peak temperatures (at  $\beta = 2 \text{ K min}^{-1}$ ) and activation energies of dehydration and decomposition processes for  $\gamma\text{-ZrPphenCu}$

Step	Process	$T$ (K)	$E$ ( $\text{kJ mol}^{-1}$ )	
			From K method	From OFW method (range of $\alpha$ )
I	Dehydration	319.9	$97 \pm 4$	$94 \pm 9$ (0.05–0.20) $102 \pm 3$ (0.20–0.65) $92 \pm 6$ (0.65–0.95)
II	Dehydration	360.5	$100 \pm 4$	$106 \pm 8$ (0.05–0.95)
III	Dehydration	407.6	$124 \pm 4$	$126 \pm 3$ (0.05–0.90) $133 \pm 5$ (0.90–0.95)
IV	Dehydration	579.4	$145 \pm 7$	$130 \pm 7$ (0.05–0.15) $139 \pm 4$ (0.15–0.95)
V	Decomposition	749.5	$180 \pm 4$	$173 \pm 6$ (0.05–0.15) $182 \pm 3$ (0.15–0.80) $176 \pm 2$ (0.80–0.95)

Temperature uncertainties are less than 0.5 K.

while the corresponding decomposition rate seems to be higher ( $\Delta E$  is about  $10 \text{ kJ mol}^{-1}$ ).

#### 4.4.4. $\gamma\text{-TiPphen}$

Three dehydration steps occur for  $\gamma\text{-TiPphen}$  between 320 and 680 K (Fig. 6). The loss of the more thermally stable coordination water along with condensation water of the orthophosphate groups occurs in the range 520–700 K. Comparable  $E$  values were found for the first two steps (between 76 and  $82 \text{ kJ mol}^{-1}$ , see Table 5), while activation energies obtained with both methods for the third step are comparable with those found for  $\gamma\text{-ZrPphen}$  (between 130 and  $144 \text{ kJ mol}^{-1}$ ).

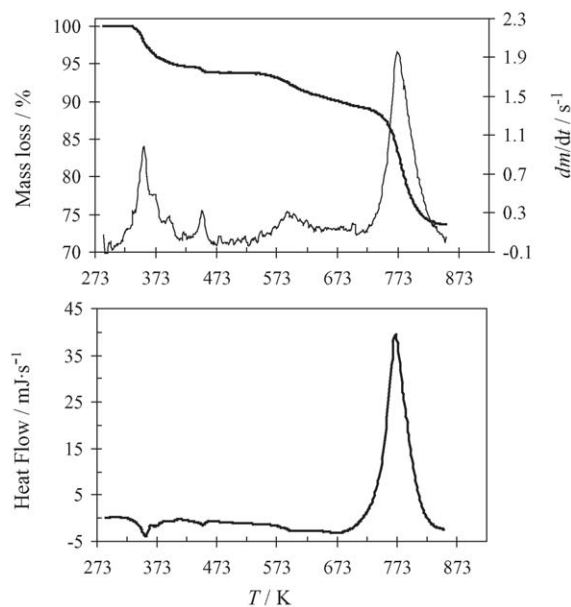


Fig. 6. TG/DTG and DSC curves of  $\gamma\text{-TiPphen}$  at  $2 \text{ K min}^{-1}$  under a stream of air.

Table 5

DSC peak temperatures (at  $\beta = 2 \text{ K min}^{-1}$ ) and activation energies of dehydration and decomposition processes for  $\gamma$ -TiPphen

Step	Process	$T$ (K)	$E$ (kJ mol $^{-1}$ )	
			From K method	From OFW method (range of $\alpha$ )
I	Dehydration	355.3	$76 \pm 2$	$76 \pm 4$ (0.05–0.95)
II	Dehydration	452.5	$78 \pm 2$	$82 \pm 3$ (0.05–0.60) $102 \pm 8$ (0.60–0.95)
III	Dehydration	599.3	$137 \pm 5$	$130 \pm 6$ (0.05–0.15) $144 \pm 4$ (0.15–0.95)
IV	Decomposition	775.9	$206 \pm 7$	$194 \pm 6$ (0.05–0.25) $203 \pm 2$ (0.25–0.60) $196 \pm 4$ (0.60–0.95)

Temperature uncertainties were less than 0.5 K for all the presented data.

A single decomposition process due to the release of phen is accompanied by an exothermic DSC peak ( $-849 \pm 7 \text{ kJ mol}^{-1}$ ) between 700 and 850 K. The OFW method gives  $E$  ( $194$ – $206 \text{ kJ mol}^{-1}$ ) while  $206 \pm 7 \text{ kJ mol}^{-1}$  was found with the Kissinger method.

#### 4.4.5. $\gamma$ -TiPphenCu

Three dehydration steps of mass loss are shown in Fig. 7 for  $\gamma$ -TiPphenCu with an overall mass loss of about 8% by weight (about 7% for  $\gamma$ -TiPphen is shown in Fig. 3). The loss of condensation water to form the pyrophosphate groups occurs at higher temperatures compared with  $\gamma$ -TiPphen (Table 2) while no relevant differences were found between the other DTG dehydration peak temperatures of  $\gamma$ -TiPphenCu and  $\gamma$ -TiPphen. A noticeable increase in activation energy (about  $100 \text{ kJ mol}^{-1}$ ) is found in comparison with that of  $\gamma$ -TiPphen (Table 6). Moreover, no activation

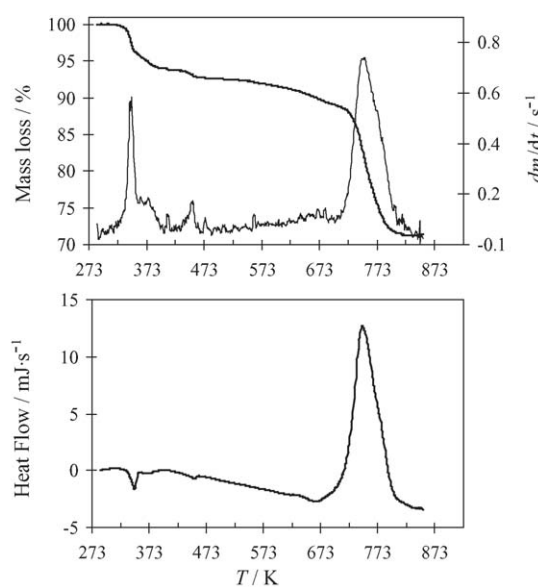


Fig. 7. TG/DTG and DSC curves of  $\gamma$ -TiPphenCu at  $2 \text{ K min}^{-1}$  under a stream of air.

Table 6

DSC peak temperatures (at  $\beta = 2 \text{ K min}^{-1}$ ) and activation energies of dehydration and decomposition processes for  $\gamma$ -TiPphenCu

Step	Process	$T$ (K)	$E$ (kJ mol $^{-1}$ )	
			From K method	From OFW method (range of $\alpha$ )
I	Dehydration	347.9	$119 \pm 4$	$125 \pm 8$ (0.05–0.25) $127 \pm 8$ (0.25–0.45) $94 \pm 9$ (0.45–0.95)
II	Dehydration	380.5	$108 \pm 4$	$80 \pm 6$ (0.05–0.30) $97 \pm 5$ (0.30–0.55) $109 \pm 3$ (0.55–0.95)
III	Dehydration	451.8	$237 \pm 9$	$233 \pm 7$ (0.05–0.40) $248 \pm 9$ (0.40–0.75) $229 \pm 9$ (0.75–0.80)
IV	Dehydration	673.7	– <sup>a</sup>	– <sup>a</sup>
V	Decomposition	754.2	$165 \pm 4$	$155 \pm 8$ (0.05–0.25) $167 \pm 3$ (0.25–0.85) $160 \pm 1$ (0.85–0.95)

Temperature uncertainties were less than 0.5 K for all the presented data.

<sup>a</sup>  $E$  values not evaluable due to a strong superimposition of steps IV and V at high heating rates.

energy values were obtained for the third step due to the strong overlap with the decomposition process at higher heating rates ( $6$  and  $8 \text{ K min}^{-1}$ ). The decomposition step ( $680$ – $850 \text{ K}$ ) takes place at lower temperature (compared to  $\gamma$ -TiPphen) and the corresponding enthalpy of  $-1300 \pm 12 \text{ kJ mol}^{-1}$  was higher than that of  $\gamma$ -TiPphen. By contrast, the corresponding decomposition rate seems to be much higher ( $\Delta E$  is about  $40 \text{ kJ mol}^{-1}$ ).

## 5. Conclusions

As a result of the present study it was found that vaporization of phen is described by a single step of mass loss with negligible variation of activation energy. Vaporization enthalpy agrees well with the mean value of  $E$  obtained from the isoconversional method. By contrast, thermal dehydration and decomposition processes of  $\gamma$ -ZrPphen,  $\gamma$ -ZrPphenCu,  $\gamma$ -TiPphen and  $\gamma$ -TiPphenCu follow multi-step kinetics. Phen decomposes from  $\gamma$ -ZrPphen at higher temperature compared to  $\gamma$ -TiPphen while decomposition of phenCu complex occurs at higher temperature for  $\gamma$ -TiPphenCu (compared to  $\gamma$ -ZrPphenCu). Hence, the difference in thermal behavior of phen and phenCu can be ascribed to the nature of the exchanger, being the content of phen and Cu comparable. Kinetic analysis of dehydration and decomposition processes greatly contributes to completely define the thermal stability of these materials, which maintain a layered structure up to  $650$ – $670 \text{ K}$ . For this reason, they can be used in some industrial processes as heterogeneous catalysts because intercalation of the phenCu complex (which exhibits a good catalytic activity) avoids its decomposition and enables it to be used at higher temperatures.

## Acknowledgements

Authors are grateful to the National Research Council of Italy (CNR) and the Italian M.U.R.S.T. for their financial supports.

## References

- [1] A. Clearfield, in: A. Clearfield (Ed.), *Inorganic Ion-Exchange Materials*, vol. 20, CRC Press, Boca Raton, FL, 1982 (Chapter 1).
- [2] C. Ferragina, A. La Ginestra, M.A. Massucci, P. Patrono, A.A.G. Tomlinson, *J. Chem. Soc. Chem. Commun.* 15 (1984) 1204.
- [3] (a) C. Ferragina, A. La Ginestra, M.A. Massucci, P. Patrono, A.A.G. Tomlinson, *J. Phys. Chem.* 89 (1985) 4762;  
(b) C. Ferragina, A. La Ginestra, M.A. Massucci, P. Patrono, A.A.G. Tomlinson, *J. Chem. Soc. Dalton Trans.* 2 (1986) 265;  
(c) C. Ferragina, A. La Ginestra, M.A. Massucci, P. Patrono, A.A.G. Tomlinson, *Mater. Res. Bull.* 22 (1987) 29.
- [4] (a) P. Giannoccaro, S. Doronzo, C. Ferragina, in: H.U. Blaser, A. Baiker, R. Prins (Eds.), *Heterogeneous Catalysis and Fine Chemicals IV*, Elsevier Science, New York, 1997, p. 633;  
(b) P. Giannoccaro, E. De Giglio, M. Gargano, M. Aresta, C. Ferragina, *J. Mol. Catal. A* 157 (1–2) (2000) 131.
- [5] C. Ferragina, M.A. Massucci, A.A.G. Tomlinson, *J. Chem. Soc. Dalton Trans.* 4 (1990) 1191.
- [6] S. Vyazovkin, C.A. Wight, *J. Phys. Chem. A* 101 (1997) 8279.
- [7] M.E. Brown, D. Dollimore, A.K. Galwey, *Reactions in the Solid State. Comprehensive Chemical Kinetics*, vol. 22, Elsevier, Amsterdam, 1980.
- [8] J. Sestak, *Thermophysical Properties of Solids, Comprehensive Analytical Chemistry*, vol. 12 D, Elsevier, Amsterdam, 1984.
- [9] S. Vyazovkin, C.A. Wight, *Anal. Chem.* 72 (2000) 3171.
- [10] M.E. Brown, M. Maciejewski, S. Vyazovkin, R. Nomen, J. Sempere, A. Burnham, J. Opfermann, R. Strey, H.L. Anderson, A. Kemmler, R. Keuleers, J. Janssens, H.O. Desseyn, C.-R. Li, T.B. Tang, B. Roduit, J. Malek, T. Mitsuhashi, *Thermochim. Acta* 355 (2000) 125.
- [11] S. Vyazovkin, *Thermochim. Acta* 355 (2000) 155.
- [12] S. Vyazovkin, N. Sbirrazzuoli, *Macromol. Chem. Phys.* 200 (1999) 2294.
- [13] T. Ozawa, *Bull. Chem. Soc. Jpn.* 38 (1965) 1881.
- [14] J.H. Flynn, L.A. Wall, *J. Res. Natl. Bur. Standards A Phys. Chem.* 70A (1966) 487.
- [15] N. Sbirrazzuoli, Y. Girault, L. Elègant, *Thermochim. Acta* 293 (1997) 25.
- [16] H.E. Kissinger, *Anal. Chem.* 29 (1957) 1702.
- [17] H.E. Kissinger, *J. Res. Natl. Bur. Standards* 57 (1956) 217.
- [18] R.G. Patel, M.M. Choudhri, *Thermochim. Acta* 25 (1978) 247.
- [19] D.J. Whelan, R.J. Spear, R.W. Read, *Thermochim. Acta* 80 (1984) 149.
- [20] S. Yamanaka, M. Tanaka, *J. Inorg. Nucl. Chem.* 41 (1979) 45.
- [21] S. Allulli, C. Ferragina, A. La Ginestra, M.A. Massucci, N. Tomassini, *J. Inorg. Nucl. Chem.* 39 (1977) 1043.
- [22] C. Ferragina, M.A. Massucci, A.A.G. Tomlinson, P. Patrono, A. La Ginestra, P. Cafarelli, in: I.V. Mitchell (Ed.), *Pillared Layered Structures*, Elsevier Applied Science, London/New York, 1990, p. 127.
- [23] C. Ferragina, A. La Ginestra, M.A. Massucci, P. Cafarelli, P. Patrono, A.A.G. Tomlinson, in: P.A. Williams, M.J. Hudson (Eds.), *Recent Developments in Ion Exchange*, vol. 2, Elsevier Applied Science, London/New York, 1990, p. 103.
- [24] M. Arfelli, G. Mattogno, C. Ferragina, M.A. Massucci, *J. Incl. Phenom. Mol. Recogn. Chem.* 11 (1991) 15.
- [25] G. Alberti, U. Costantino, E. Torracca, *J. Inorg. Nucl. Chem.* 28 (1966) 225.